Accepted Manuscript

Evaporation of ethanol/water mixture droplets on pillar-like PDMS surface

Ying-Song Yu[1]*, Sun Li[1], Xianfu Huang[2, 3], Jin-Zhi Zhou[1]*

1. Department of Mechanics, School of Civil Engineering, Architecture and Environment, Hubei University of Technology, Wuhan 430068, China

2. State Key Laboratory of Nonlinear Mechanics, Institute of Mechanics, Chinese Academy of Sciences, Beijing 100190, China

3. School of Engineering Science, University of Chinese Academy of Sciences, Beijing 100049, China

Corresponding authors. E-mail: yuys@hbut.edu.cn (Y.S. Yu), hgzhongzhou@126.com (Z.J. Zhou).

Graphical abstract
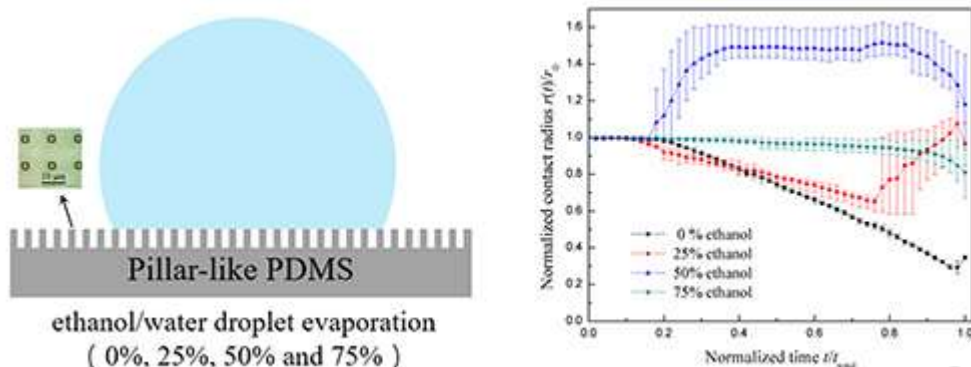
Abstract

Evaporation of about 6 μL ethanol/water droplet with different ethanol concentrations on both planar and pillar-like polydimethylsiloxane (PDMS) surfaces was experimentally studied. It was found that a small fraction of the as-fabricated pillar-like PDMS surface was Wenzel-wetted while other part Cassie-Baxter-wetted. When ethanol/water droplet evaporates on planar PDMS surface, the contact radius continuously decreases with time, and the contact angle first increase to a maximum, then keeps unchanged and finally decreases, which is different from that of pure water droplet. However, when mixture droplet evaporates on pillar-like PDMS surface, without or with the addition of ethanol, the droplet first experiences a relatively long constant contact radius (CCR) stage. Moreover, it was observed that there is a spreading process at the final stage of mixture droplet with 25% ethanol. More interesting is that when 50% ethanol/water droplet evaporates on pillar-like PDMS surface, the contact radius continuously increases at the end of CCR stage, and the contact angle nearly keep unchanged for a relatively long period when the contact radius increases to a maximum. To better understand the spreading behavior, a microscopy was used to record the process from the top and it was found that the solid-liquid area developed to an octagon. The average spreading speed was measured to be 0.3-0.9 μm/s. Using Taylor's expansion theorem, the excess free energy was calculated and it is concluded that evaporating droplet will spontaneously spread on pillar-like PDMS surface when

the excess energy becomes larger than the energy barrier.

Introduction

Evaporation is an omnipresent phenomenon and it has found applications in many fields such as pesticide spraying, spray cooling, combustion, ink-jet printing, micro-/nano-fluidics and lab-on-a-chip. Due to contact angle hysteresis [1], the contact line of evaporating water droplet is pinned at first for a certain time and such a phenomenon is named as constant contact area mode or constant contact radius mode (CCR) by Picknett and Bexon [2]. When the contact angle decreases to the receding angle, the contact line begins to recede while contact angle almost keeps unchanged corresponding to constant contact angle mode [2]. Finally, droplet evaporates completely with decrease of both contact radius and contact angle, *viz.*, mixed mode. The three different evaporation modes have been reported and intensively studied by many scholars [3-8]. When a sessile droplet evaporates on a hydrophilic surface, due to the high evaporation flux near the three-phase contact line, there will be a capillary flow, which drivies the liquid from inside to the contact line to compensate the liquid loss resulting in the pinning of the contact line [9-10]. Meanwhile, there is a temperature gradient because of the difference of evaporation flux and a Marangoni flow will be consequently induced [11-15]. However, for the case of hydrophobic or superhydrophobic surfaces, it has been reported that a reverse flow comes into being [16, 17]. Besides, evaporation of water droplet on pillar-like [18-23] and microline-like [24] surfaces has also been intensively studied.

As an example of the applications of droplet evaporation, if micro-/nano-particles are introduced into the droplet, these particles will be left on the substrates as liquid evaporates completely. Usually, a coffee-ring-like structure will be observed because the compensation flow will continuously carry these particles to the edge, which limits the application of droplet evaporation. This phenomenon is called coffee-ring effect [9] and different pinning mechanisms of micro-/nano-particles have been set up [25-31]. To better application of evaporative deposition, a lot of methods including varying the particle shape [32] and evaporation environment [33], applying electric field [34, 35],

4

adding surfactants [36] or polymer additives [37], promoting particle adsorption and long-range interaction [38] are used to suppress coffee-ring effect. For more details on coffee-ring effect, please refer to the references [39-42].

At room environment, evaporation of sessile droplet is usually a very slow process, which may limit the application of droplet evaporation. One of the best choices may be to use binary droplet. During the latest decades, more attention has been paid to evaporation of ethanol/water mixture droplet [43-51]. Besides, ethylene glycol [52] or methanol [53] /water droplets have also been experimentally studied. Since these organic solvents usually have strong volatility and a solvent diffuses quickly to the liquid-vapor interface than another one, evaporation of mixture droplet behavior more complex than that of pure droplet. The contact radius usually recedes at the beginning while contact angle increases. When the contact angle approaches to a maximum, it keeps almost unchanged. Finally, droplet evaporates completely with decreasing of both contact radius and contact angle. Moreover, evaporation of sessile binary droplet is more complex because of the flow inside it [48, 49, 51].

In this paper, we experimentally studied evaporation of ethanol-water mixture droplets on both planar and pillar-like PDMS surfaces. We found that addition of ethanol and microstructures of surfaces have great influence on the evaporative characteristics. More interesting is that when 50% ethanol/water droplet evaporates on pillar-like PDMS surfaces, the contact line is pinned at first, then the contact line continuously advances on the surface to achieve a maximum of projection area, and finally, the area keeps unchanged until complete evaporation. Similar spreading phenomenon is also found at the final stage of mixture droplet with initial ethanol concentration of 25%. We estimated the average spreading speed of 50% ethanol/water droplet and concluded that it was the excess free energy that induced spontaneous spreading of evaporating mixture droplet on pillar-like PDMS surface.

Experiments

Silicon master with microstructures was prepared by photolithography. It was first

ultrasonically stirred in ethanol and acetone for about 10 min, respectively, to ensure that the surface is clean. After oxygen plasma (Harrick PDC-002 setup) for 5 minutes, the clean silicon was further modified by a self-assembled chlorotrimethylsilane (Aladdin) monolayer to further minimize its surface energy. Polydimethylsiloxane (PDMS, Sylgard 184, Dow corning, USA) whose mass ratio of base to curing agent is 10:1 was mixed completely and vacuumed for about 30 minutes to ensure that all the visible bubbles have been extracted. Then the PDMS was poured onto the patterned silicon master and spin-coated at the rate of ~650 rpm for 18 s and it was vacuumed for 30 minutes to extract all the bubbles between the polymer and the silicon master. After thermal curing at 90 ℃ for about 3 hours, a regular pillar-like PDMS substrate was obtained by peeling off the PDMS mold from the patterned silicon master. The microstructure of the pillar-like PDMS substrate is illustrated in Fig. 1. The pillar width d and height h are 10 and 20 μm, respectively. The pillar to pillar distance w is 26 μm.
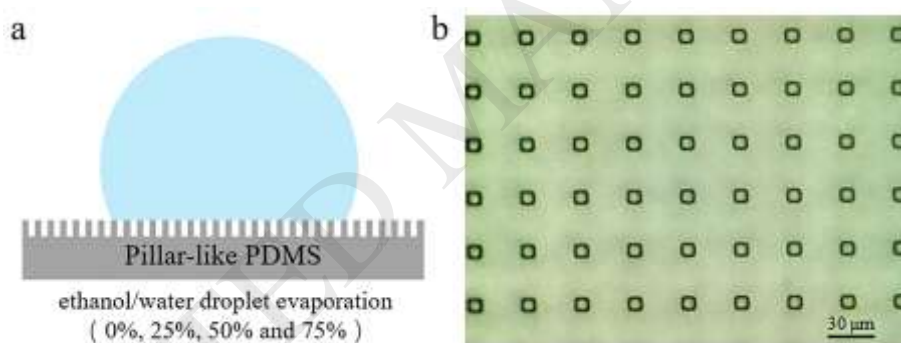

Fig. 1. Mixture droplet evaporating on pillar-like PDMS surface. **a** schematic, **b** image of PDMS substrate with 10 μm×10 μm pillars separated by a distance 26 μm.

About 6.0 μL ethanol/water mixture droplets (the volume concentration of ethanol is 0%, 25%, 50% and 75%) were slightly deposited on patterned PDMS substrate and observed using OCA20 system (precision: ±0.1°, Dataphysics, Germany) equipped with a high-resolution camera at 0.5 fps. The environmental temperature and relatively humidity are 27.3±2 ℃ and 34±3%, respectively. Moreover, 6 μL 50 v/v% ethanol/water mixture droplet was observed from top view using Hirox KH-8700 microscopy (Japan) at temperature of 26.8±1 ℃ and relative humidity of 48±2%. Images were obtained at

6

the time interval of 5 s. All experiments were repeated at least six times to ensure the reproducibility. Following the method suggested by Huhtamäki et al. [54], the advancing and receding contact angles of pure water droplet are measured using DSA30 system (precision: $\pm 0.1°$, Krüss, Germany) at temperature of $23\pm1\,℃$ and relative humidity of 29±2%. The advancing and receding contact angles of water droplet on planar PDMS surface are, respectively, $118.39\pm2°$ and $96.83\pm2°$, while those on pillar-like PDMS surface are, respectively, $158.24\pm2°$ and $137.62\pm2°$. Since ethanol has a strong volatility, the advancing and receding contact angles of mixture droplets and pure ethanol droplet on both planar and pillar-like PDMS surfaces are not measured.

Results and discussion

Table 1. Analysis of initial contact angles of evaporating droplets on PDMS surfaces.

ethanol concentration	θ_0	θ_1	θ_W	θ_C	χ
0%	111.84°	148.90°	126.98°	162.11°	0.272
25%	95.48°	145.68°	98.88°	158.49°	0.135
50%	67.56°	133.05°	51.89°	153.33°	0.140
75%	34.77°	86.19°	0°	149.29°	0.272

Table 1 shows the initial contact angles of mixture droplets on planar or pillar-like PDMS surfaces. θ_0 and θ_1 are, respectively, the initial contact angle of mixture droplets on planar and regular pillar-like PDMS surfaces. If it follows the Wenzel model [55], the fraction of solid-liquid interface is $f = 1 + \dfrac{4dh}{(d+w)^2} = 1.617$. If Cassie-Baxter model [56] is valid, the fraction of solid-vapor area is defined as $f_{sv} = 1 - \dfrac{d^2}{(d+w)^2} = 0.923$ and the fraction of solid-liquid interface f_{sl} is 0.077.

Using the above two models, the values of the Wenzel contact angle θ_W and Cassie one θ_C are calculated and listed in Table 1. It is found that the actual contact angles all range between those predicted by the two models, indicating that some liquid penetrates into

the gaps among the micropillars but did not wet the bottom. Then a mixed wetting mode, $\cos\theta_M = \chi\cos\theta_W + (1-\chi)\cos\theta_C$, suggested by Zheng *et al.* [57], was used to predict the wettability of mixture droplet. Here, χ is a parameter describing the fraction of the patterned surface which is Wenzel-wetted and $(1-\chi)$ is the fraction of the patterned surface which is Cassie-Baxter-wetted. The values of χ were listed in Table 1, indicating that for the pillar-like PDMS surface, a small part of the patterned surface was Wenzel-wetted while the other surface was Cassie-Baxter-wetted without or with the addition of ethanol. In the above analysis, the effect of gravity on droplet shape was ignored. Besides, pure ethanol droplet was not analyzed because it completely spreads on the regular pillar-like PDMS surface.
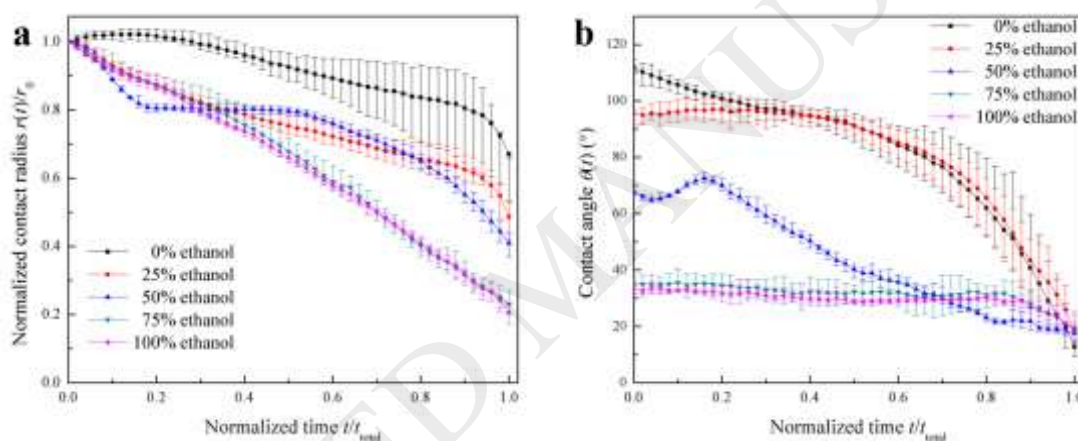

Fig. 2. Evolution of contact radius and contact angle of evaporating water droplets on planar PDMS surfaces. **a** normalized contact radius, **b** contact angle.

Fig. 2 illustrated the evolution of the normalized contact radius and contact angle of evaporating mixture droplets on planar PDMS surface (time dependent changes of normalized contact radius and contact angle were given in Figure S1 in the Appendix), indicating that addition of ethanol has great influence on evaporation of mixture droplet. The values of normalized contact radius and contact angle are all averaged. And the error bars are obtained by calculating the difference between the maximum/minimum and the average. For pure water droplet, constant contact radius mode (CCR) scaled about 20% and then the evaporation switched to constant contact angle mode and ended with mixed mode. As 25% ethanol was added into the mixture droplet, the contact

8

radius decreased throughout the whole process, while the contact angle kept almost nearly unchanged for about 40% of the total evaporation time and then decreased with time. For 50% ethanol-water mixture droplet, at first the contact radius decreased with time while the contact angle decreased first and then increased to a maximum. Then the contact radius kept unchanged for about 30% of the total evaporation time. Finally, both the contact radius and contact angle decreased with time. For 75% ethanol-water mixture droplet and pure ethanol droplet, evaporation both began with CCA stage which scaled about 80% of the total evaporation time and ended with mixed mode. For pure ethanol droplet, it was found that the contact angle was nearly constant, which is consistent with the experiments by Shanahan et al. [58, 59]. Moreover, Shanahan et al. [59] pointed out that it is attributed to little pinning of the contact line.

Fig. 3 shows the evolution of normalized contact radius and contact angle of evaporating mixture droplet on pillar-like PDMS surface (time dependent changes of normalized contact radius and contact angle were given in Figure S2 in the Appendix), which is different from those on planar PDMS surface. For pure water droplet and 25% ethanol-water mixture droplet, the evaporation proceeds first with a short stage of CCR mode, then switches to CCA which dominated during the whole process, and finally ends with mixed mode. Moreover, for mixture droplet with ethanol concentration of 25%, there was an explicit spreading process at the final stage and at the beginning of spontaneous propagation there is an explicit collapse indicating the spontaneous spreading as shown in Fig. 3 and Fig.4. For 50% ethanol-water mixture droplet, the contact radius kept unchanged for about 20% of the total evaporation time, then it spread on pillar-like PDMS surface. When the contact radius increased to the maximum, it switched to CCR stage for half of the total evaporation time and finally ended with mixed mode. For 75% ethanol-water mixture droplet, CCR stage dominated and scaled about 80% and finally the droplet evaporated with mixed mode. Besides, pure ethanol droplet on pillar-like PDMS surface was not investigated because it spread quickly and completely.
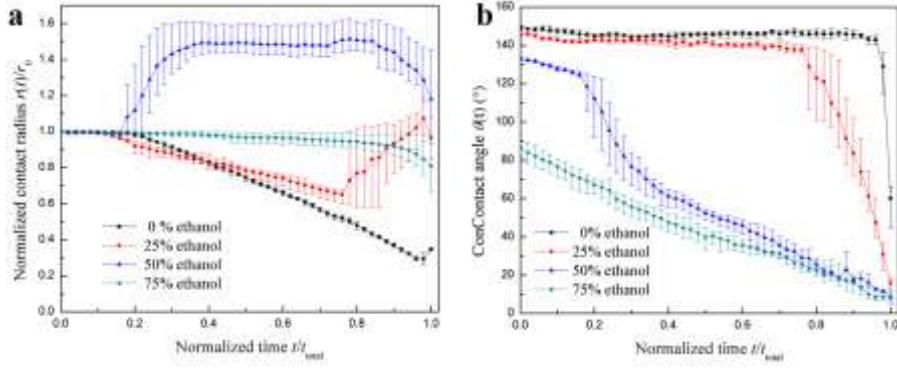
9

Fig 3. Evolution of contact radius and contact angle of ethanol/water droplets evaporating on pillar-like PDMS surfaces. **a** normalized contact radius, **b** contact angle.
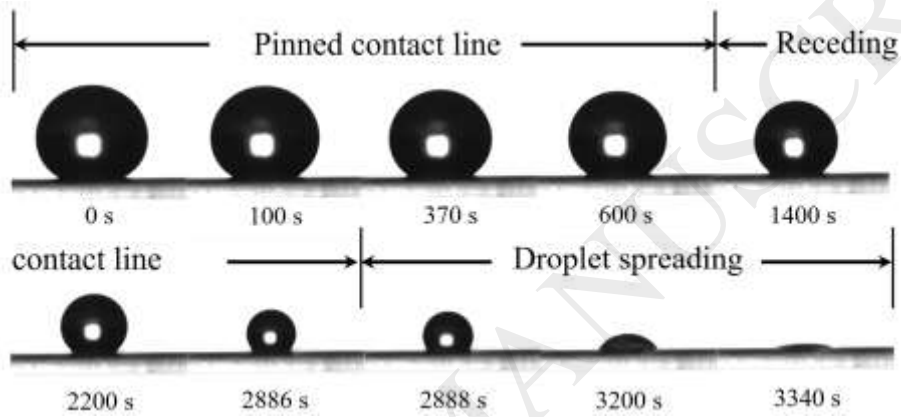

Fig. 4. Evaporation of 25% ethanol/water mixture droplet.

Especially, for pure water droplet on pillar-like PDMS surface, the diffusion coefficient can be obtained using the following equation [18]

$$\frac{D\Delta ct}{\rho_L r_0^2} - k = -\frac{\tilde{r}^2}{2}\left[\frac{-0.721171}{1+\cos\theta} + 0.164791\ln\left(1+\cos\theta\right) + 0.113804\cos\theta + 0.044559\cos^2\theta\right] \tag{1}$$

where $\tilde{r} = r/r_0$, r_0 and r are, respectively, the initial and spontaneous contact radii. ρ_L is the density of liquid, k is a constant. D and Δc are, respectively, the diffusion coefficient and vapor concentration difference. Combining Eq. (1) with the data in Fig. 3, the diffusion coefficient-vapor concentration difference product can be obtained from Fig. 5 if the initial contact radius and the vapor concentration difference are both known.
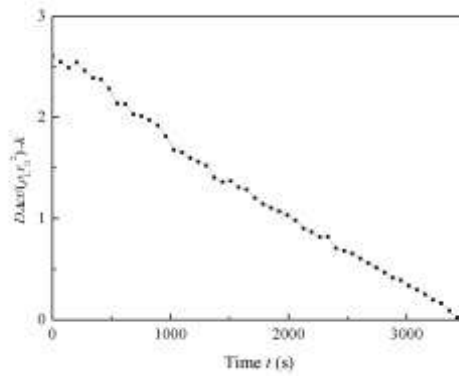
Fig. 5. Diffusion coefficient-vapor diffusion difference product for pure water droplet

evaporating on pillar-like PDMS surface.

Fig. 6 illustrated the evaporation of 50% ethanol-water mixture droplet from top view

using Hirox KH-8700 microscopy. Because the contact angle is much larger than 90°,

the contact line cannot be observed. However, at about 200 s, there is a sudden change

of droplet profile indicating the transition from mixed mode state to Wenzel state. From

then on, the liquid continuously propagates on patterned PDMS surface and the solid-

liquid interface had a shape of an octagon. Similar phenomenon is also found in

References [60-62]. At 200 s, 495 s and 850 s, the side-to-side distances are measured

to be, respectively, 3.06, 3.60, and 3.84 mm. Assuming droplet spreads uniformly, the

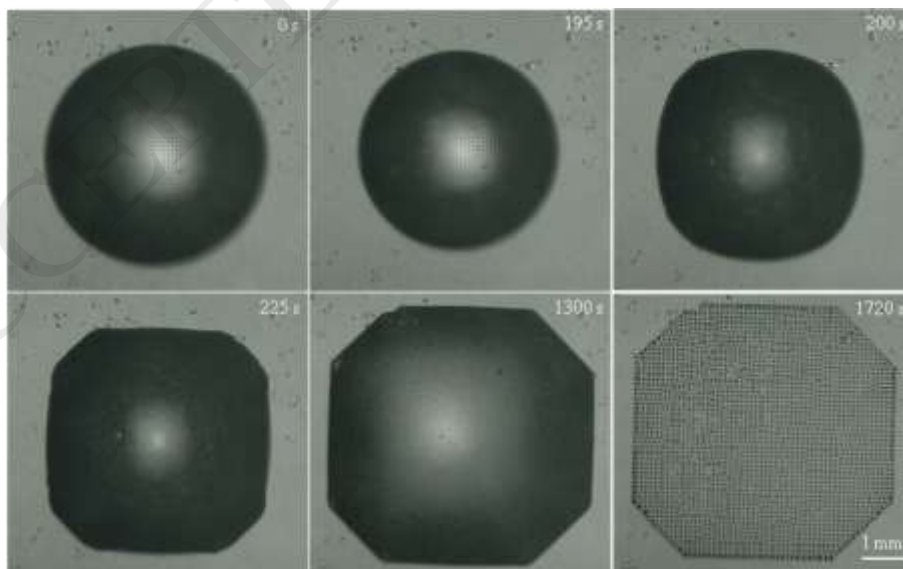average spreading speed is of the order of 0.3-0.9 μm/s.

Fig. 6. Images of evaporating droplet with initial ethanol concentration of 50% viewed

11

from top view.

Why is there a long-time spreading process at the final stage of evaporating mixture droplet with initial ethanol concentration of 25%? Why does the same behavior happen during evaporation of 50% ethanol/water droplet? In 1995, Shanahan [63] set up a theory of stick-slip phenomenon and it was later used to explain the stick-slip behavior of evaporating droplet [64-66]. Here, we modified this theory to explain the spontaneous spreading of evaporating droplet. For simplicity, we neglected the gravity effect and proposed that mixture droplet has a shape of spherical cap. Moreover, the liquid volume penetrating into the pillars is too small to be calculated. Then the droplet volume is given as

$$V = \frac{\pi r^3}{3\sin^3\theta}(1-\cos\theta)^2(2+\cos\theta) \tag{2}$$

The liquid/vapor interfacial area $A_{LV}^{(1)}$ above the pillars and that between the pillars $A_{LV}^{(2)}$ are, respectively, given as

$$A_{LV}^{(1)} = \frac{2\pi r^2}{1+\cos\theta} \tag{3}$$

$$A_{LV}^{(2)} = (1-\chi)\left[1 - \frac{d^2}{(d+w)^2}\right]\pi r^2 \tag{4}$$

The solid/liquid one A_{SL} are given as

$$A_{SL} = \chi\pi r^2 + \frac{4\chi dh}{(d+w)^2}\pi r^2 + (1-\chi)\frac{d^2}{(d+w)^2}\pi r^2 \tag{5}$$

The interfacial Gibbs free energy of mixture droplet can be written as

$$\begin{aligned} G &= A_{LV}^{(1)}\gamma_{LV}^{(1)} + A_{LV}^{(2)}\gamma_{LV}^{(2)} + A_{SL}\gamma_{SL} - A_{SV}\gamma_{SV} \\ &= A_{LV}^{(1)}\left(\gamma_{LV}^{(1)} - \gamma_{LV}^{(2)}\right) + \left(A_{LV}^{(1)} + A_{LV}^{(2)}\right)\gamma_{LV}^{(2)} + \left[\chi\pi r^2 + \frac{4\chi dh}{(d+w)^2}\pi r^2 + (1-\chi)\frac{d^2}{(d+w)^2}\pi r^2\right]\left(\gamma_{SL} - \gamma_{SV}\right) \end{aligned} \tag{6}$$

where $\gamma_{LV}^{(1)}$, $\gamma_{LV}^{(2)}$, γ_{SL} and γ_{SV} are, respectively, the liquid/vapor (above the pillars), liquid/vapor (between pillars), solid/liquid and solid/vapor interfacial tensions. Considering that ethanol evaporates quickly from the liquid-vapor interface and there is not enough ethanol diffusing from inside the droplet to the liquid-vapor interface to compensate the loss of ethanol, the ethanol concentration at the liquid-vapor interface will be less than that inside the droplet, resulting in $\gamma_{LV}^{(1)} > \gamma_{LV}^{(2)}$.

For mixture droplet on patterned surface as mentioned above, the mixed mode

12

equation is valid for equilibrium condition as

$$\cos\theta_e = \chi\left[1+\frac{4dh}{(d+w)^2}\right]\cos\theta_Y + (1-\chi)\left[\frac{d^2}{(d+w)^2}\cos\theta_Y - 1 + \frac{d^2}{(d+w)^2}\right] \tag{7}$$

where $\gamma_{SV} - \gamma_{SL} = \gamma_{LV}^{(2)}\cos\theta_Y$.

Combining Eq. (6) with Eq. (7), the Gibbs free energy of mixture droplet can be given as

$$G = \pi r^2\left(\frac{2\gamma_{LV}^{(1)}}{1+\cos\theta} - \gamma_{LV}^{(2)}\cos\theta_e\right) \tag{8}$$

At constant droplet volume, the following relationship can be obtained from Eq. (2) as

$$\frac{d\theta}{dr} = \frac{-\sin\theta(2+\cos\theta)}{r} \tag{9}$$

When the mixture droplet is slightly out of equilibrium, for example, with the increase of contact radius r_e, *viz.*, $r = r_e + \delta r$ and the corresponding contact angle can be given as $\theta = \theta_e - \delta\theta$. Using Taylor's expansion theorem, the excess Gibbs free energy of the mixture droplet can be expressed as

$$\delta G = G(r_e + \delta r) - G(r_e) = \delta r\left[\frac{dG}{dr}\right]_{r=r_e} + 0\left[(\delta r)^2\right] \tag{10}$$

Making use of Eq. (8)-(10), the excess Gibbs free energy can be given as

$$\delta G = G(r_e + \delta r) - G(r_e) = \delta r\left[\frac{dG}{dr}\right]_{r=r_e} \approx 2\pi\left[\gamma_{LV}^{(1)} - \gamma_{LV}^{(2)}\right]\delta r\cos\theta_e \tag{11}$$

When the contact angle θ_e is larger than 90° and the contact radius r continuously increases, δG will decrease as δr. When there is enough energy to overcome the energy barrier, the contact line will spontaneously spread to a new equilibrium.

Conclusion

Evaporation of ethanol-water mixture droplets on both planar and pillar-like PDMS surfaces were experimentally studied. It was found that addition of ethanol and microstructure have great influence on evaporation of mixture droplets. Moreover, we found that the droplet will spontaneously spread at final stage of evaporating mixture droplet with initial ethanol concentration of 25%. Similar phenomenon is also found in evaporation of mixture droplet with initial ethanol concentration of 50% at the end of CCR stage. The average spreading speed of 50% ethanol/water droplet was estimated.

13

Under the assumption of spherical droplet, the excess Gibbs free energy of mixture droplet was calculated using Taylor's expansion theorem and it was found that the spontaneous spreading of mixture droplet with initial concentration of 25% and 50% is induced when such excess free energy becomes larger than the energy barrier.

Acknowledgments

References

[1] H.B. Eral. Contact angle hysteresis: a review of fundamentals and applications. *Colloid Polym. Sci.* 291 (2013) 247-260.

[2] R.G. Picknett, R. Bexon. The evaporation of sessile or pendant drops in still air. *J. Colloid Interf. Sci.* 61 (1977) 336-350.

[3] H. Hu, R.G. Larson. Evaporation of a sessile droplet on a substrate. *J. Phys. Chem. B* 106 (2002) 1334-1344.

[4] C. Poulard, G. Guéna, A.M. Cazabat. Diffusion-driven evaporation of sessile drops. *J. Phys.: Condens. Matter* 17 (2005) S4213.

[5] Y.S. Yu, Z.Q. Wang, Y.P. Zhao. Experimental and theoretical investigations of evaporation of sessile water droplet on hydrophobic surfaces. *J. Colloid Interf. Sci.* **365** (2012) 254-259

[6] Y.S. Yu, Z.Q. Wang, Y.P. Zhao. Experimental study of evaporation of sessile water

droplet on PDMS surfaces. *Acta Mech. Sin.* **29** (2013) 799-805.

[7] M.C. Lopes, E. Bonaccurso. Evaporation control of sessile water drops by soft viscoelastic surfaces. *Soft Matter* **8** (2012) 7875-7881.

[8] H.Y. Erbil. Evaporation of pure liquid sessile and spherical suspended drops: a review. *Adv. Colloid Interf. Sci.* **170** (2012) 67-86.

[9] R.D. Deegan, O. Bakajin, T.F. Dupont, G. Huber, S.R. Nagel, T.A. Witten. Capillary flow as the cause of ring stains from dried liquid drops. *Nature* **389** (1977) 827-829.

[10] H. Hu, R.G. Larson. Analysis of the microfluid flow in an evaporating sessile droplet. *Langmuir* **21** (2005) 3963-3971.

[11] H. Hu, R.G. Larson. Analysis of the effects of Marangoni stresses on the microflow in an evaporating sessile droplet. Langmuir 21 (2005) 3972-3980.

[12] X.F. Xu, J.B. Luo. Marangoni flow in an evaporating water droplet. *Appl. Phys. Lett.* **91** (2007) 124102.

[13] X.F. Xu, J.B. Luo, D. Guo. Criterion for reversal of thermal Marangoni flow in drying drops. *Langmuir* **26** (2009) 1918-1922.

[14] F. Girard, M. Antoni, K. Sefiane. On the effect of Marangoni flow on evaporation rates of heated water drops. *Langmuir* 24 (2008) 9207-9210.

[15] Z.Q. Wang, Y.P. Zhao. In situ observation of thermal Marangoni convection on the surface of a sessile droplet by infrared thermal imaging. *J. Adhes. Sci. Technol.* **26** (2012) 2177-2188.

[16] Z.H. Pan, S. Dash, J.A. Weibel, S.V. Garimella. Assessment of water droplet evaporation mechanisms on hydrophobic and superhydrophobic substrates. *Langmuir* 29 (2013) 15831-15841.

[17] S. Dash, A. Chandramohan, S.V. Garimella. Flow visualization during droplet evaporation on hydrophobic and superhydrophobic surfaces. *J. Heat Transfer* **136** (2014) 080917.

[18] G. McHale, S. Aqil, N.J. Shirtcliffe, M.I. Newton, H.Y. Erbil. Analysis of droplet evaporation on a superhydrophobic surface. *Langmuir* **21** (2005) 11053-11060.

15

[19] N. Anantharaju, M. Panchagnula, S. Neti. Evaporating drops on patterned surfaces: transition from pinned to moving triple line. *J. Colloid Interf. Sci.* **337** (2009) 176-182.

[20] X.M. Chen, R.Y. Ma, J.T. Li, C.L. Hao, W. Guo, B.L. Luk, S.C. Li, S.H. Yao, Z.K. Wang. Evaporation of droplets on superhydrophobic surfaces: surface roughness and small droplet size effects. *Phys. Rev. Lett.* **109** (2012) 116101.

[21] W. Xu, R. Leeladhar, Y.T. Kang, C.H. Choi. Evaporation kinetics of sessile water droplets on micropatterned superhydrophobic surfaces. *Langmuir* **29** (2013) 6032-6041.

[22] C. Zhang, X.L. Zhu, L.W. Zhou. Morphology tunable pinning force and evaporation modes of water droplets on PDMS spherical cap micron-arrays. *Chem. Phys. Lett.* **508** (2011) 134-138.

[23] Y.C. Chuang, C.K. Chu, S.Y. Lin, L.J. Chen. Evaporation of water droplets on soft patterned surfaces. *Soft Matter* **10** (2014) 3394-3403.

[24] C. Luo, M.M. Xiang, X.C. Liu. Transition from Cassie-Baxter to Wenzel states on micronline-formed PDMS surfaces induced by evaporation or pressing of water droplets. *Microfluid Nanofluid* **10** (2011) 831-842.

[25] J.Y. Jung, Y.W. Kim, J.Y. Yoo, J. Koo, Y.T. Kang. Forces acting on a single particle in an evaporating sessile droplet on a hydrophilic surface. *Anal. Chem.* **82** (2010) 784-788.

[26] T.S. Wong, T.H. Chen, X. Shen, C.M. Ho. Nanochromatography driven by the coffee ring effect. *Anal. Chem.* **83** (2011) 1871-1873.

[27] V.H. Chhasatia, Y. Sun. Interaction of bi-dispersed particles with contact line in an evaporating colloidal drop. *Soft Matter* **7** (2011) 10135-10143.

[28] B.M. Weon, J.H. Je. Self-pinning by colloids confined at a contact line. *Phys. Rev. Lett.* **110** (2013) 028303.

[29] Y.Q. Li, H.A. Wu, F.C. Wang. Effect of a single nanoparticle on the contact line motion. *Langmuir* **32** (2016) 12676-12685.

[30] Y.S. Yu, X.L. Xia, X. Zheng, X.F. Huang, J.Z. Zhou. Quasi-static motion of microparticles at the depinning contact line of evaporating droplet on PDMS surfaces. *Sci.China Phys. Mech. Astron.* **60** (2017) 094612.

[31] Y.S. Yu, M.C. Wang, X.F. Huang. Evaporative deposition of polystyrene microparticles on PDMS surface. *Sci. Rep.* **7** (2017) 14118.

[32] P.J. Yunker, T. Still, M.A. Lohr, A.G. Yodh. Suppression of the coffee-ring effect by shape-dependent capillary interactions. *Nature* **476** (2011) 308-311.

[33] M. Majumder, C.S. Rendall, J.A. Eukel, J.Y.L. Wang, N. Bahabtu, C.L. Pint, T.Y. Liu, A.W. Orbaek, F. Mirri, J. Nam, A.R. Barron, R.H. Hauge, H.K. Schmidt, M. Pasquali. Overcoming the "coffee-stain" effect by compositional Marangoni-flow-assisted drop-drying. *J. Phys. Chem. B* **116** (2012) 6536-6542.

[34] H.B. Eral, D.M. Augustine, M.H.G. Duits, F. Mugele. Suppressing the coffee stain effect: how to control colloidal self-assembly in evaporating drops using electrowetting. *Soft Matter* 7 (2011) 4954-4958.

[35] D. Mampallil, H.B. Eral, D. van den Ende, F. Mugele. Control of evaporating complex fluids through electrowetting. *Soft Matter* **8** (2012) 10614-10617.

[36] T. Still, P.J. Yunker, A.G. Yodh. Surfactant-induced Marangoni eddies alter the coffee-rings of evaporating colloidal drops. *Langmuir* **28** (2012) 4984-4988.

[37] L.Y. Cui, J.H. Zhang, X.M. Zhang, L. Huang, Z.H. Wang, Y.F. Li, H.N. Gao, S.J. Zhu, T.Q. Wang, B. Yang. Suppression of the coffee ring effect by hydrosoluble polymer additives. *ACS Appl. Mater. Interf.* **4** (2012) 2775-2780.

[38] A. Crivoi, F. Duan. Elimination of the coffee-ring effect by promoting particle adsorption and long-range interaction. *Langmuir*, **29 (2013)** 12067-12074.

[39] Z.Q. Lin. *Evaporative Self-assembly of Ordered Complex Structures.* World Scientific Publishing Co. Pte. Ltd. Singapore, 2012.

[40] Y. P. Zhao. *Physical Mechanics of Surfaces and Interfaces.* Science Press, Beijing, 2012.

[41] K. Sefiane. Patterns from drying drops *Adv. Colloid Interf.* **206** (2014) 372-381.

17

[42] D. Mampallil, H.B. Eral. A review on suppression and utilization of the coffee-ring effect. *Adv. Colloid Interf.* **252 (2018)** 38-54.

[43] K. Sefiane, L. Tadrist, M. Douglas. Experimental study of evaporating water-ethanol mixture sessile drop: influence of concentration. *Int. J. Heat Mass Transfer*. **46** (2003) 4527-4534.

[44] C.J. Liu, E. Bonaccurso, H.J. Butt. Evaporation of sessile water/ethanol drops in a controlled environment. *Phys. Chem. Chem. Phys.* **10** (2008) 7150-7157.

[45] Z. Wang, X.F. Peng, A.S. Mujumdar, A. Su, D.J. Lee. Evaporation of ethanol-water mixture drop on horizontal substrate. *Dry. Technol.* **26** (2008) 806-810.

[46] L.X. Shi, P. Shen, D. Zhang, Q.L. Lin, Q.C. Jiang. Wetting and evaporation behaviors of water-ethanol sessile drops on PTFE surfaces. *Surf. Interface Anal.* **41 (2009)** 951-955.

[47] C.H. Ooi, E. Bormashenko, A.V. Nguyen, G.M. Evans, D.V. Dao, N.T. Nguyen. Evaporation of ethanol–water binary mixture sessile liquid marbles. *Langmuir* **32** (2016) 6097-6104.

[48] J.R. Christy, Y. Hamamoto, K. Sefiane. Flow transition within an evaporating binary mixture sessile drop. *Phys. Rev. Lett.* **106** (2011) 205701.

[49] Y. Hamamoto, J.R.E. Christy, K. Sefiane. The flow characteristics of an evaporating ethanol water mixture droplet on a glass substrate. *J. Therm. Sci. Tech-Jpn* **7** (2012) 425-436.

[50] T. Ozturk, H.Y. Erbil. Evaporation of water-ethanol binary sessile drop on fluoropolymer surfaces: influence of relative humidity. Colloid Surf. A 553 (2018) 327-336.

[51] M.H. He, H.H. Qiu. Internal flow patterns of an evaporating multicomponent droplet on a flat surface. *Int. J. Therm. Sci.* **100** (2016) 10-19.

[52] M. Rusdi, Y. Moroi, H. Nakahara, O. Shibata. Evaporation from water-ethylene glycol liquid mixture. *Langmuir* **21** (2005) 7308-7310.

[53] K. Sefiane, S. David, M.E.R. Shanahan. Wetting and evaporation of binary mixture

drops. *J. Phys. Chem. B* **112** (2008) 11317-11323.

[54] T. Huhtamäki, X. Tian, J.T. Korhonen, R.H.A. Ras. Surface-wetting characterization using contact-angle measurements. *Nature Protoc.* **13** (2018) 1521-1538.

[55] R.N. Wenzel. Resistance of solid surfaces to wetting by water. *Ind. Eng. Chem.* **28** (1936) 988-994.

[56] A.B.D. Cassie, S. Baxter. Wettability of porous surfaces. *Trans. Faraday Soc.* **40** (1944) 546-551.

[57] Q.S. Zheng, Y. Yu, Z.H. Zhao. Effects of hydraulic pressure on the stability and transition of wetting modes of superhydrophobic surfaces. *Langmuir* **21** (2005) 12207-12212.

[58] J.R. Moffat, K. Sefiane, M.E.R. Shanahan. Effect of TiO2 Nanoparticles on contact line stick-slip behavior of volatile drops. *J. Phys. Chem. B* **113** (2009) 8860-8866.

[59] M.E.R. Shanahan, K. Sefiane, J.R. Moffat. Dependence of volatile droplet lifetime on the hydrophobicity of the substrate. *Langmuir* **27** (2011) 4572-4577.

[60] Q.Z. Yuan, Y.P. Zhao. Wetting on flexible hydrophilic pillar-arrays. *Sci. Rep.* **3** (2013) 1944.

[61] Q.Z. Yuan, Y.P. Zhao. Multiscale dynamic wetting of a droplet on a lyophilic pillar-arrayed surface. *J. Fluid Mech.* **716** (2013) 171-88.

[62] Q.Z. Yuan, X.F. Huang, Y.P. Zhao. Dynamic spreading on pillar-arrayed surfaces: viscous resistance versus molecular friction. *Phys. Fluids* **26** (2014) 092104.

[63] M.E.R. Shanahan. Simple theory of "stick-slip" wetting hysteresis. *Langmuir* **11** (1995) 1041-1043.

[64] D. Orejon, K. Sefiane, M.E.R. Shanahan. Stick-slip of evaporating droplets: substrate hydrophobicity and nanoparticle concentration. *Langmuir* **27** (2011) 12834-12843.

[65] A. Askounis, K. Sefiane, V. Koutsos, M.E.R. Shanahan. The effect of evaporation kinetics on nanoparticle structuring within contact line deposits of volatile drops.

Colloids Surf. A **441** (2014) 855-866.

[66] M. Oksuz, H.Y. Erbil. Comments on the energy barrier calculations during "stick-slip" behavior of evaporating droplets containing nanoparticles. *J. Phys. Chem. C* **118** (2014) 9228-9238.

Table

Table 1. Analysis of initial contact angles of evaporating droplets on PDMS surfaces.

ethanol concentration	θ_0	θ_1	θ_W	θ_C	χ
0%	111.84°	148.90°	126.98°	162.11°	0.272
25%	95.48°	145.68°	98.88°	158.49°	0.135
50%	67.56°	133.05°	51.89°	153.33°	0.140
75%	34.77°	86.19°	0°	149.29°	0.272

Figure captions

Figure 1. Mixture droplet evaporating on pillar-like PDMS surface. **a** schematic, **b** Image of PDMS substrate with 10 μm×10 μm pillars separated by a distance 26 μm.

Figure 2. Evolution of contact radius and contact angle of evaporating water droplets on planar PDMS surfaces. **a** normalized contact radius, **b** contact angle.

Figure 3. Evolution of contact radius and contact angle of ethanol/water droplets evaporating on pillar-like PDMS surfaces. **a** normalized contact radius, **b** contact angle.

Figure 4. Evaporation of 25% ethanol/water mixture droplet.

Figure 5. Images of evaporating droplet with initial ethanol concentration of 50% viewed from top view.